HHS Public Access

Author manuscript

Nat Med. Author manuscript; available in PMC 2012 June 01.

Published in final edited form as:

Nat Med. ; 17(12): 1685–1691. doi:10.1038/nm.2554.

Cancer Cell-Selective *In Vivo* Near Infrared Photoimmunotherapy Targeting Specific Membrane Molecules

Makoto Mitsunaga, **Mikako Ogawa**, **Nobuyuki Kosaka**, **Lauren T. Rosenblum**, **Peter L Choyke**, and **Hisataka Kobayashi***

Molecular Imaging Program, Center for Cancer Research, National Cancer Institute, National Institutes of Health, Bethesda, Maryland 20892-1088, USA

Abstract

Three major modes of cancer therapies, surgery, radiation and chemotherapy, have been the mainstay of modern oncologic therapy. To minimize side effects, molecular targeted cancer therapies including armed antibody therapy have been developed with limited success. In this study, we developed a new type of molecular targeted cancer therapy, photoimmunotherapy (PIT), employing a target-specific photosensitizer based on a near infrared (NIR) phthalocyanine dye, IR700, conjugated to monoclonal antibodies (MAb) targeting epidermal growth factor receptors (EGFR). Cell death was induced immediately only upon irradiating, MAb-IR700 bound, target cells with NIR light. *In vivo* tumor shrinkage after irradiation with NIR light was observed only in target EGFR-expressing cells. The MAb-IR700 conjugates were most effective when bound to the cell membrane, producing no phototoxicity when not bound, suggesting a different mechanism for PIT compared with conventional photodynamic therapies. Target selective PIT enables treatment of cancer based on MAb binding on the cell membrane.

In order to minimize the side effects of conventional cancer therapies, including surgery, radiation and chemotherapy, molecular targeted cancer therapies have been developed. Among the existing targeted therapies, monoclonal antibodies (MAb) therapy have the longest history, and to date, over 25 therapeutic MAbs have been approved by the Food and Drug Administration (FDA)[1,2]. Effective MAb therapy traditionally depends on three mechanisms: antibody-dependent cellular cytotoxicity (ADCC), complement-dependent cytotoxicity (CDC), and receptor blockade and requires multiple high doses of the MAb. MAbs have also been used at lower doses as vectors to deliver therapies such as radionuclides[3] or chemical or biological toxins[4]. Ultimately, however, dose limiting toxicity relates to the biodistribution and catabolism of the antibody conjugates.

Correspondence should be addressed to: Hisataka Kobayashi, M.D., Ph.D., Molecular Imaging Program, Center for Cancer Research, National Cancer Institute, NIH, Building 10, Room B3B69, MSC1088, Bethesda, MD 20892-1088. Phone: 301-451-4220; Fax: 301-402-3191; kobayash@mail.nih.gov.

Author Contributions: M.M. conducted experiments, performed analysis and wrote the manuscript; M.O., N.K. and L.T.R conducted experiments and performed analysis; P.L.C. wrote the manuscript and supervised the project; and H.K. planned and initiated the project, designed and conducted experiments, wrote the manuscript, and supervised the entire project.

Conventional photodynamic therapy (PDT), which combines a photosensitizing agent with the physical energy of non-ionizing light to kill cells, has been less commonly employed for cancer therapy because the current non-targeted photosensitizers are also taken up in normal tissues, thus, causing serious side effects, although the excitation light itself is harmless in the near infrared (NIR) range (Fig. 1). Were it feasible to design a highly targeted photosensitizer, toxicity could be greatly reduced. Although the targeted photosensitizer may distribute throughout the body, it will only be active where intense light is applied, reducing the likelihood of off-target effects. Most existing photosensitizers are poorly selective small molecules which bind not only to cancer cells but also to normal cells including the skin and other epithelial surfaces resulting in unwanted phototoxicity. These agents are generally hydrophobic, therefore, permeate into cells and produce reactive oxygen species intracellularly, leading to cell death. Thus, target specific delivery of conventional photosensitizers is theoretically difficult because, after reaching the cell, the agent must still be internalized into organelles, such as mitochondria, to be most effective. Various combinations of conventional photosensitizers and MAbs have been tested to improve selectivity with limited success especially when measured by *in vivo* therapeutic effects[5-11]. There are several reasons for unsuccessful outcomes; 1. Conventional photosensitizers have low extinction coefficients that requires conjugation of large numbers of photosensitizers to a single antibody molecule thus, potentially decreasing binding affinity. 2. Conventional photosensitizers are mostly hydrophobic leading to difficulties in conjugating photosensitizers to antibodies without compromising the immunoreactivity and *in vivo* target accumulation. 3. Conventional photosensitizers generally absorb light in the visible range reducing tissue penetration.

In this study, we develop a MAb-based photosensitizer, which is activated by NIR light for targeted photoimmunotherapy (PIT), only when bound to the target molecule on the cancer cellular membrane. Further, because this agent also emits a diagnostic fluorescence, it can be used to direct the application of light to minimize light exposure to non-relevant tissues and non-invasively monitor therapeutic effects.

Results

In vitro characterization of MAb-IR700 conjugates

Conjugation of trastuzumab, a MAb directed against human epidermal growth factor receptor 2 (HER2), or panitumumab, a MAb directed against human epidermal growth factor receptor (HER1), to IRDye 700DX N-hydroxysuccinimide (NHS) ester (IR700) resulted in ~3 IR700 molecules conjugated to each MAb molecule. The trastuzumab-IR700 (Tra-IR700) and panitumumab-IR700 (Pan-IR700) preparations demonstrated strong association and contained no detectable MAb aggregates as determined by high performance liquid chromatography (HPLC) and sodium dodecyl sulfate polyacrylamidegel elctrophoresis SDS-PAGE (Supplementary Fig. 1a, b). *In vitro* immunoreactivity of MAb-IR700 conjugates were analyzed with a binding assay using ^{125}I-labeled MAb-IR700 conjugates, and revealed that 73.38 ± 0.39% (^{125}I-Tra-IR700) and 78.61 ± 0.89% (^{125}I-Pan-IR700) of binding was achieved with each MAb conjugate respectively and the specificity of binding was confirmed by blocking with excess native unconjugated MAb (less than 1.4%)

(Supplementary Fig. 1c). Since immunoreactivity of ^{125}I-Tra and ^{125}I-Pan measured with the same method were 78 ± 2%, and 82 ± 3%, respectively, minimal loss of MAbs with IR700 conjugation was confirmed.

MAb-IR700 mediated phototoxicity leads rapidly to necrotic cell death *in vitro*

Fluorescence microscopy was performed to visualize the cellular binding location of the conjugates. Consistent with previous studies, IR700 fluorescence was detected mainly on the cell surface of 3T3/HER2 cells, which express HER2 protein, after 1 h incubation at 4 °C with Tra-IR700, whereas the fluorescence was also detected inside the cells after 6 h incubation at 37 °C with Tra-IR700, indicating gradual internalization[12] (Fig. 2a). Co-staining with LysoTracker-Green revealed co-localization of IR700 with the endolysosomal compartment (Fig. 2b). After 1 h and 6 h of incubation with Tra-IR700, excitation light (fluorescence microscope; power density of 2.2 mW cm^{-2}) induced fluorescence as well as cellular swelling, bleb formation, and rupture of vesicles representing necrotic cell death (Fig. 2c and Supplementary Video 1a, b). Necrotic cell death was also observed using HER1 positive A431 cells incubated with Pan-IR700 which were exposed to excitation light as described above (Fig. 3a).

To further explore the nature of the phototoxicity of Tra-IR700 on 3T3/HER2 cells we used the LIVE/DEAD assay to analyze acute phototoxicity and trypan blue dye exclusion assay to analyze the effect on proliferation. As cell death was induced rapidly upon irradiation (Supplementary Video 1a, b), the LIVE/DEAD assay, which can detect the cells with damaged membranes was performed within 1 h after the treatment. The percentage of cell death in target cells vs. untreated control cells was significantly influenced by excitation light dose (Fig. 2d). In addition, there was no significant cytotoxicity associated with exposure to Tra-IR700 without excitation light or with light exposure without Tra-IR700. Similar results were obtained for A431 cells with Pan-IR700 (Fig. 3b), however, panitumumab itself had a noticeable treatment effect against A431 cells due to down regulation and signal inhibition of HER1[13]. In addition, parental 3T3 cells served as HER2 receptor-negative controls, therefore, we chose 3T3/HER2 cells with Tra-IR700 for further *in vitro* study. Proliferation assay revealed that long term growth inhibition was confirmed only when cells were treated with Tra-IR700 and exposed to light (Fig. 2e, f and Supplementary Fig. 2a).

Target-specific phototoxic cell death induced only when MAb-IR700 is bound to the target membrane antigen

There was no significant difference in phototoxicity between 1 h and 6 h incubation with Tra-IR700 (Fig. 2g), indicating that membrane binding of Tra-IR700 was sufficient to induce cell death. When Tra-IR700 was localized to the endolysosomal compartment (Fig. 2b), it also induced rupture of the vesicle with cellular swelling and bleb formation after irradiation (Supplementary Video 1a). However, this did not appear to be a major cause of cell death, since cell death could be observed without endolysosomal localization of Tra-IR700 within 1 h of incubation at 4 °C (Supplementary Video 1b). Interestingly, failure to wash the cells prior to irradiation did not influence the phototoxic effect indicating that cellular membrane binding was important to the phototoxic effects of the conjugate, not

merely the presence of the conjugate. Further, the IR700 dye alone (200 nM; equivalent IR700 concentration of Tra-IR700 conjugates) did not incorporate into the cells or induce phototoxcity in cells (Fig. 2h and Supplementary Fig. 2b). Additionally, phototoxcity was dose-dependently blocked by the excess unconjugated trastuzumab (Supplementary Fig. 2c, d). Furthermore, Tra-IR700 did not induce therapeutic effect to A431 cells (Fig. 2i). These results confirm that cell death is dependent on specific membrane binding of Tra-IR700.

To confirm that the phototoxicity was target specific, we next treated 3T3/HER2 and Balb/3T3/DsRed, which is a parental HER2 negative Balb/3T3 transfected with DsRed fluorescent protein. Tra-IR700 was distributed in a HER2 specific manner while DsRed expressing Balb/3T3 cells did not show phototoxicity upon irradiation (Fig. 4a and Supplementary Video 2). In addition, LIVE/DEAD Green staining demonstrated HER2 specific induction of cell death as determined by multi-color fluorescence microscopy (Fig. 4b) and flowcytometry analysis (Fig. 4c). Target-specific phototoxicity was also confirmed with Pan-IR700 mediated PIT in A431 cells and Balb/3T3/DsRed (HER1 negative) co-cultured cells (Fig. 3c). Overall, Tra-IR700 and Pan-IR700 showed identical therapeutic effects to HER2 positive (3T3/HER2) and HER1 positive (A431) cells, respectively, except that unconjugated panitumumab showed noticeable growth inhibition but unconjugated trastzumab did not reduce growth with the dose used.

Role of reactive oxygen species on Tra-IR700 mediated photoimmunotherapy

Reactive oxygen species (ROS) have been implicated in the cell death associated with conventional PDT. To clarify the role of photon-induced redox reactions (e.g. singlet oxygen ($^1O_2$)) in producing phototoxicity with Tra-IR700, a redox quencher, sodium azide (NaN_3)[14], was added to the medium when cells were irradiated. The percentage of cell death was partially decreased in the presence of sodium azide, in a dose dependent manner (Fig. 2j).

Target specific accumulation of MAb-IR700 *in vivo*

To examine the conjugate distribution *in vivo*, we prepared a xenograft tumor model bearing A431 (HER1 positive) and 3T3/HER2 (HER1 negative) tumors in each dorsum of a mouse. A431 tumors were visualized with IR700 fluorescence 1 d after intravenous injection of Pan-IR700 (50 μg) (Fig. 5a). The fluorescence intensity of Pan-IR700 in a A431 tumor decreased gradually over days, while tumor to background ratios (TBRs) increased (Fig. 5b, c). The fluorescence intensity of the 3T3/HER2 tumor was the same as that of background (non-tumor lesions). When 300 μg of Pan-IR700 was administered intravenously, fluorescence intensity of the A431 tumor was more than 3 times higher than 50 μg injection at 1 d after injection, however, TBR was lower because of high background signal (Fig. 5b, c). As less antitumor activity was found in mice receiving 50 μg (vs. 300 μg) of Pan-IR700 injection following irradiation (Supplementary Fig. 3), therefore, we chose the higher injection dose for the treatment study. Biodistribution of Tra-IR700 was determined with IR700 fluorescence because tissue levels of radioactivity and fluorescence might be different due to their different excretion routes and catabolism when using dual-labeled radiolabeled-Pan-IR700[15]. There was no other specific localization of IR700 except for bladder

accumulation on day 1 probably due to excretion of catabolized and unbound dye (Fig. 5d, and Supplementary Fig. 4a).

Target-specific tumor shrinkage in response to MAb-IR700 mediated photoimmunotherapy

A431 tumors were treated with a single dose of light at 1 d after Pan-IR700 administration. The efficacy of Pan-IR700 mediated PIT was studied in 8 groups of A431 tumor bearing mice (at least $n = 12$ mice in each group). All treated tumors were less than 500 mm^3 as larger tumors were associated with side effects (i.e. subcutaneous bleeding, tumor bleeding or weakened state) requiring euthanasia in accordance with our institution's animal care and use guidelines. Tumor volume was significantly reduced in A431 tumors treated with Pan-IR700 PIT compared with non treatment control mice (Fig. 5e), and survival was significantly prolonged in Pan-IR700-PIT treated mice (Fig. 5f). No significant therapeutic effect was observed in other control groups of mice. Similar results were obtained in 3T3/HER2 tumors treated with Tra-IR700 PIT (Supplementary Fig. 4b). Pathological analysis revealed that only scant viable A431 tumor cells were present after Pan-IR700 mediated PIT and massive granulation with inflammatory change was observed in the tumor nodule (Fig. 5g). It was also observed that tissue edema developed superficially. To assess the acute phase toxicity of Pan-IR700, we repeatedly administrated 300 μg of Pan-IR700 intravenously twice a week for 4 w, but there were no adverse effects observed up to 8 w ($n = 4$) compared with the control group.

Discussion

Conventional PDT for cancer therapy is based on the preferential accumulation of a photosensitizer in tumor to produce phototoxicity with minimal damage to surrounding tissue[16]. Traditionally, PDT is thought to be mediated by the generation of ROS, especially singlet oxygen, in the presence of oxygen[16]. However, to the extent that existing photosensitizers lack tumor selectivity, considerable damage can be seen in normal tissues leading to dose limiting toxicity. Thus, current methods of PDT would be improved if more selective targeting of the photosensitizer and more efficient phototoxicity per photon absorbed was possible.

Various combinations of conventional photosensitizers and MAbs have been tested to improve selectivity[5-11]. Although a large number of photosensitizers have been evaluated, IR700 has several favorable chemical properties. Amino-reactive IR700 is a relatively hydrophilic dye and can be covalently conjugated with MAb using the NHS ester of IR700 which leads to high tumor uptake. IR700 also has more than 5–fold higher extinction coefficient (2.1×10^5 $M^{-1}cm^{-1}$ at the absorption maximum of 689 nm)[17], than conventional photosensitizers such as the hematoporphyrin derivative; Photofrin® (1.2×10^3 $M^{-1}cm^{-1}$ at 630 nm), meta-tetrahydroxyphenylchlorin; Foscan® (2.2×10^4 $M^{-1}cm^{-1}$ at 652 nm), and mono-L-aspartylchlorin e6; NPe6/Laserphyrin® (4.0×10^4 $M^{-1}cm^{-1}$ at 654 nm)[18].

The selectivity of the MAb-IR700 is derived from its activation after binding to the cell membrane of target cells; unbound conjugate does not contribute to phototoxicity (Fig. 2a, g, h). Short term viability assays, as well as long term proliferation assays, demonstrated that the conjugate was capable of inducing specific cell death (Fig. 2d–f). When co-cultures of

receptor-positive and -negative cells were treated, only the receptor-positive cells were killed despite the presence of unbound MAb-IR700 in the culture medium (Fig. 4a–c; see also Supplementary Video 2). This selective cell killing minimizes damage to normal cells.

Although the mechanism of phototoxicity with MAb-IR700 is not completely clear, the agent must be bound to the cellular membrane to be active. Treatment with sodium azide, a well known redox and singlet oxygen scavenger, only partially reduced the phototoxicity but did not totally eliminate the effectiveness of the conjugate (Fig. 2j). This indicates that ROS generation is a minor part of the phototoxic effect. The observation that phototoxicity was induced after incubation with MAb-IR700 after only 1 h at 4 °C, indicates that internalization of the conjugate is not required for activity (Fig. 2g, and Supplementary Video 1b). This differs from the current generation of PDT agents that require intracellular localization to be effective. Video microscopy demonstrated rapid visible damage to the membrane and lysosomes after exposure to light, following incubation for more than 6 h at 37 °C, when the MAb-conjugate was internalized (Supplementary Video 1a). Previous studies have indicated that intracellular uptake of MAb-photosensitizer conjugates is responsible for inducing phototoxicity[6-10]. While this new MAb-IR700 conjugate does not require internalization for phototoxic cell death, cell surface antigen binding is required (Fig. 2g, h). For instance, the rupture of endolysosome occurred within a second of light exposure (Supplementary video 1a). Cell death induced by singlet oxygen generally induces a slower apoptotic cell death (Supplementary Fig. 5a, b)[19,20]. Since cell membrane damage was so quickly induced even at 4 °C by this method, it is hypothesized that cell death is caused by the rapid expansion of locally heated water with relatively minor effects due to singlet oxygen effects (Fig.2g, j, and Supplementary video 1a, b)[21].

Another desirable feature of PIT using fluorescent MAb-IR700 conjugate is that it permitted the detection of targeted tissue. Theoretically, this would allow specific lesions to be identified with PIT rather than irradiating the entire field. Doses required for diagnosis (50 μg), however, were significantly lower than those required for therapy (300 μg) Improved intratumoral distribution of antibody occurred with the therapeutic dose (Supplementary Fig. 6)[22,23]. Because both bound and unbound agent fluoresces, there is relatively high background signal at therapeutic doses (Fig. 5a–c). Nevertheless, after PIT, the fluorescence of the treated tumors decreased and eventually disappeared, suggesting a potential means of monitoring the treatment (Fig. 5d).

One difficulty in interpreting the *in vivo* results of this study was that trastuzumab, but not panitumumab, demonstrated minor therapeutic effects by itself without the application of light. Since panitumumab is an IgG2 and trastuzumab is an IgG1, this was likely mediated by ADCC and CDC effects even though non-saturating doses were administered (Fig. 5e, f and Supplementary Fig. 4b)[24]. Based on the similarity of the phototoxicity induced with three different MAbs against several different cells expressing various numbers of respective target molecules and considering the potentially additive benefits from immunotherapy (Supplementary Fig. 7), we believe that this method may be generally applicable to other MAbs[25,26].

The NIR excitation light wavelength (peaking at 689 nm) allows penetration of at least several centimeters into tissues[16]. By using fiber-coupled laser diodes with diffuser tips, NIR light can be delivered within several centimeters of otherwise inaccessible tumors located deep to the body surface. Using such fibers, PDT has been used to treat brain tumors and peritoneal metastasis of ovarian cancer[27]. In addition to treating solid cancers it may be possible to target circulating tumor cells since they could be excited when they traverse superficial vessels. Although no toxicity was observed in our experiments, clinical translation will require formal toxicity studies. In addition, free IR700 and catabolized IR700, are readily excreted into urine within 1 hour without accumulation in any specific organ (Supplementary Fig. 8). The other component of PIT, light irradiation with NIR at 690 nm wavelength is unlikely to be toxic except at thermal doses. Theoretically, there should be no limitations on the cumulative irradiation dose of NIR light, unlike ionizing radiation such as x-ray or gamma-ray (Fig. 1). Therefore, repeated PIT might be possible for long term management of some cancer patients. In reality, repeated PIT with 3 different regimens (3 or 4 fractionated NIR irradiations at a single dose of MAb-IR700 and 4 cycles of PIT every 2 weeks after multiple doses of antibody) controlled tumor re-growth, resulting in tumor free survival of more than 4 months.

In conclusion, we have developed a target specific PIT based on MAb-IR700 conjugate (Fig. 1). The photosensitizer, IR700, is excited in the NIR range leading to deeper tissue penetration resulting in successful eradication of subcutaneously xenografted tumors after only a single dose of external NIR light irradiation. Targeted phototoxicity seems to be primarily dependent on binding of the MAb-IR700 to the cell membrane and to a lesser extent on internalization and ROS formation. The ability to covalently conjugate any number of different antibodies to IR700 means that this may be a highly flexible theranostic platform. The fluorescence induced by the conjugate can be used to non-invasively guide both PIT and monitor the results of therapy. Thus, the MAb-IR700 conjugate is a promising therapeutic and diagnostic agent for the treatment of cancer.

Supplementary Material

Refer to Web version on PubMed Central for supplementary material.

Acknowledgments

This research was supported by the Intramural Research Program of the US National Institutes of Health, National Cancer Institute, Center for Cancer Research. We would like to thank C. Regino, T. Hirano and C. Paik for their technical support.

References

1. Waldmann TA. Immunotherapy: past, present and future. Nat Med. 2003; 9:269–277. [PubMed: 12612576]
2. Reichert JM, Rosensweig CJ, Faden LB, Dewitz MC. Monoclonal antibody successes in the clinic. Nat Biotechnol. 2005; 23:1073–1078. [PubMed: 16151394]
3. Goldenberg DM, Sharkey RM, Paganelli G, Barbet J, Chatal JF. Antibody pretargeting advances cancer radioimmunodetection and radioimmunotherapy. J Clin Oncol. 2006; 24:823–834. [PubMed: 16380412]

4. Pastan I, Hassan R, Fitzgerald DJ, Kreitman RJ. Immunotoxin therapy of cancer. Nat Rev Cancer. 2006; 6:559–565. [PubMed: 16794638]
5. Mew D, Wat CK, Towers GH, Levy JG. Photoimmunotherapy: treatment of animal tumors with tumor-specific monoclonal antibody-hematoporphyrin conjugates. J Immunol. 1983; 130:1473–1477. [PubMed: 6185591]
6. Sobolev AS, Jans DA, Rosenkranz AA. Targeted intracellular delivery of photosensitizers. Prog Biophys Mol Biol. 2000; 73:51–90. [PubMed: 10781829]
7. Carcenac M, et al. Internalisation enhances photo-induced cytotoxicity of monoclonal antibody-phthalocyanine conjugates. Br J Cancer. 2001; 85:1787–1793. [PubMed: 11742503]
8. Vrouenraets MB, et al. Development of meta-tetrahydroxyphenylchlorin-monoclonal antibody conjugates for photoimmunotherapy. Cancer Res. 1999; 59:1505–1513. [PubMed: 10197621]
9. Vrouenraets MB, et al. Targeting of aluminum (III) phthalocyanine tetrasulfonate by use of internalizing monoclonal antibodies: improved efficacy in photodynamic therapy. Cancer Res. 2001; 61:1970–1975. [PubMed: 11280754]
10. Hamblin MR, Miller JL, Hasan T. Effect of charge on the interaction of site-specific photoimmunoconjugates with human ovarian cancer cells. Cancer Res. 1996; 56:5205–5210. [PubMed: 8912858]
11. Mew D, et al. Ability of specific monoclonal antibodies and conventional antisera conjugated to hematoporphyrin to label and kill selected cell lines subsequent to light activation. Cancer Res. 1985; 45:4380–4386. [PubMed: 4028022]
12. Ogawa M, Regino CA, Choyke PL, Kobayashi H. In vivo target-specific activatable near-infrared optical labeling of humanized monoclonal antibodies. Mol Cancer Ther. 2009; 8:232–239. [PubMed: 19139133]
13. Yang XD, et al. Eradication of established tumors by a fully human monoclonal antibody to the epidermal growth factor receptor without concomitant chemotherapy. Cancer Res. 1999; 59:1236–1243. [PubMed: 10096554]
14. Pooler JP, Valenzeno DP. The role of singlet oxygen in photooxidation of excitable cell membranes. Photochem Photobiol. 1979; 30:581–584. [PubMed: 538095]
15. Ogawa M, et al. Dual-Modality Molecular Imaging Using Antibodies Labeled with Activatable Fluorescence and a Radionuclide for Specific and Quantitative Targeted Cancer Detection. Bioconjugate Chemistry. 2009; 20:2177–2184. [PubMed: 19919110]
16. Dougherty TJ, et al. Photodynamic therapy. J Natl Cancer Inst. 1998; 90:889–905. [PubMed: 9637138]
17. Wilson, BC.; Patterson, MS. The determination of light fluence distributions in photodynamic therapy. In: Kessel, D., editor. Photodynamic therapy of neoplastic disease. Vol. 1. CRC; Boca Ranton: 1990. p. 129-144.
18. Detty MR, Gibson SL, Wagner SJ. Current clinical and preclinical photosensitizers for use in photodynamic therapy. J Med Chem. 2004; 47:3897–3915. [PubMed: 15267226]
19. Weishaupt KR, Gomer CJ, Dougherty TJ. Identification of singlet oxygen as the cytotoxic agent in photoinactivation of a murine tumor. Cancer Res. 1976; 36:2326–2329. [PubMed: 1277137]
20. Patterson MS, Madsen SJ, Wilson BC. Experimental tests of the feasibility of singlet oxygen luminescence monitoring in vivo during photodynamic therapy. J Photochem Photobiol B. 1990; 5:69–84. [PubMed: 2111394]
21. Thorpe WP, Toner M, Ezzell RM, Tompkins RG, Yarmush ML. Dynamics of photoinduced cell plasma membrane injury. Biophys J. 1995; 68:2198–2206. [PubMed: 7612864]
22. Kosaka N, et al. Semiquantitative assessment of the microdistribution of fluorescence-labeled monoclonal antibody in small peritoneal disseminations of ovarian cancer. Cancer Science. 2010; 101:820–825. [PubMed: 19961490]
23. Kosaka N, et al. Microdistribution of fluorescently-labeled monoclonal antibody in a peritoneal dissemination model of ovarian cancer. Proc SPIE. 2010; 7576:7576041–7576049.
24. Mandler R, Kobayashi H, Hinson ER, Brechbiel MW, Waldmann TA. Herceptin-geldanamycin immunoconjugates: pharmacokinetics, biodistribution, and enhanced antitumor activity. Cancer Res. 2004; 64:1460–1467. [PubMed: 14973048]

25. Nanus DM, et al. Clinical use of monoclonal antibody HuJ591 therapy: Targeting prostate specific membrane antigen. Journal of Urology. 2003; 170:S84–S88. [PubMed: 14610416]

26. van Dongen GA, Visser GW, Vrouenraets MB. Photosensitizer-antibody conjugates for detection and therapy of cancer. Adv Drug Deliv Rev. 2004; 56:31–52. [PubMed: 14706444]

27. Zhong W, et al. In vivo high-resolution fluorescence microendoscopy for ovarian cancer detection and treatment monitoring. Br J Cancer. 2009; 101:2015–2022. [PubMed: 19920823]

28. Euhus DM, Hudd C, LaRegina MC, Johnson FE. Tumor measurement in the nude mouse. J Surg Oncol. 1986; 31:229–234. [PubMed: 3724177]

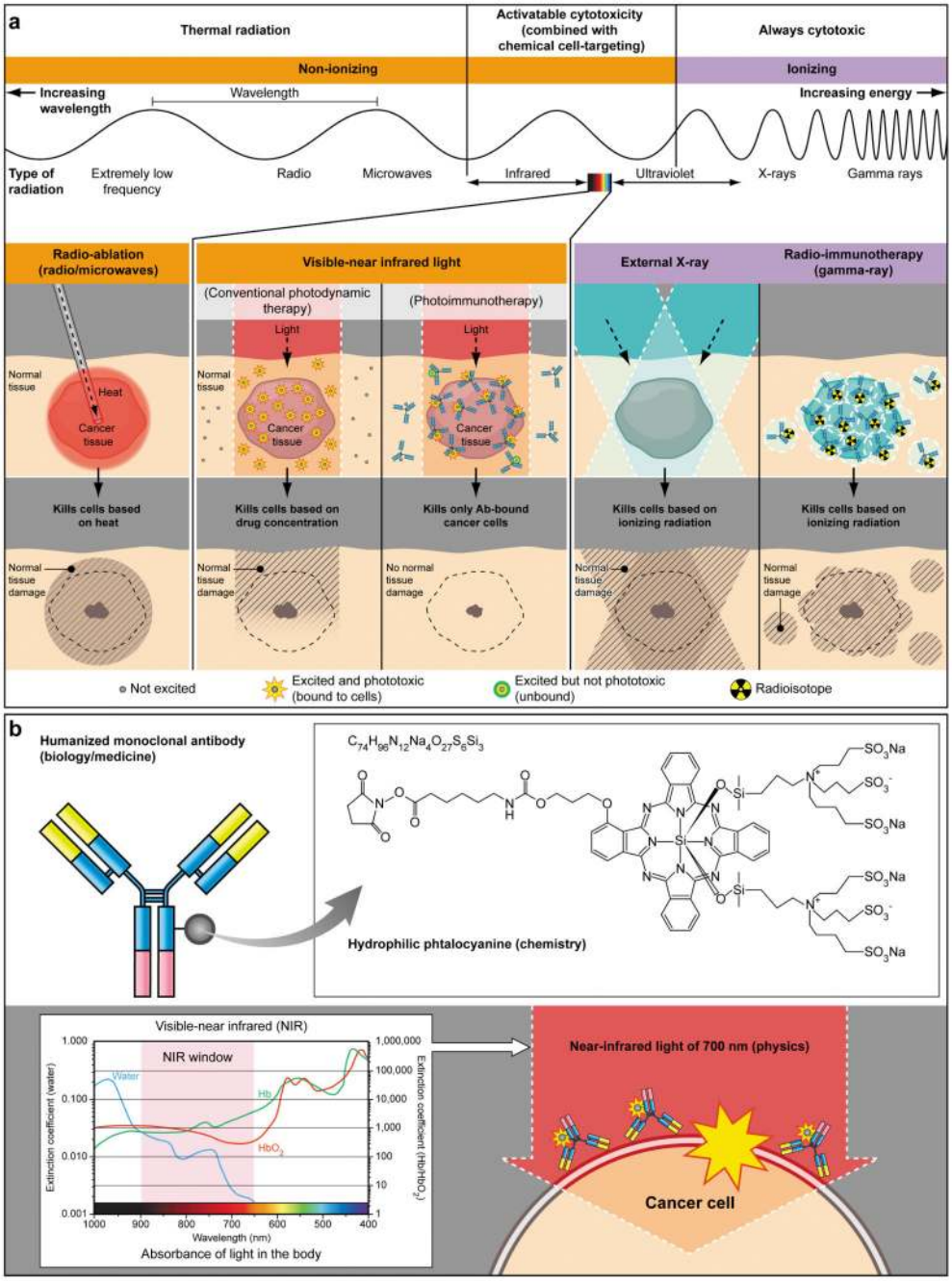

Figure 1.

(**a**) A schema for explaining selective cancer therapy with photoimmunotherapy (PIT) in the context of other physical cancer therapies employing electro-magnetic wave irradiation. Although other physical cancer therapies induce different types of damages in the normal tissue, PIT dedicatedly damages cancer cells without damaging normal cells or tissues. (**b**) A schema for explaining photo-physical, chemical and biological basis of PIT. Humanized antibodies are employed as a delivary vehicle from the biology and medicine points of view because of its highest binding specificity, greatest *in vivo* target delivery, low

immunogenecity among the clinically applicable targeting reagents. A hydrophilic phtalocyanine is employed as a activatable cytotoxic “Nano-dynamite” reagent from the chemistry points of view because of its great absorption of near infrared light of 700nm and strong cytotoxicity induced only when associating with the cell membrane. Near infrared light of 700nm is employed as an initiator for activating cytotoxicity from the physics points of view because of its high energy among non-harmful non-ionizing photons and great *in vivo* tissue penetration.

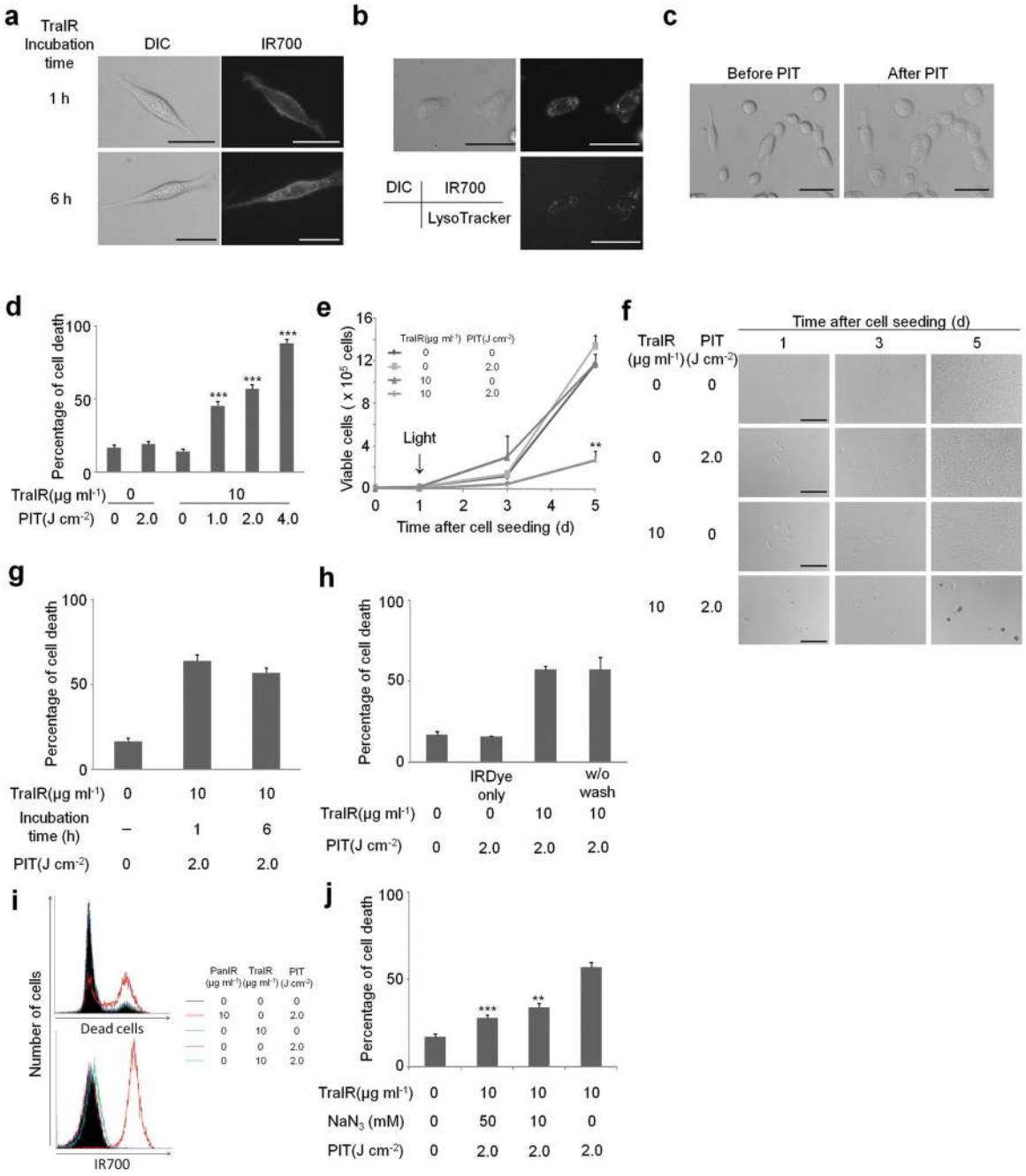

Figure 2. Target specific cell death in response to Tra-IR700 mediated photoimmunotherapy for 3T3/HER2 cells

(**a**) Different subcellular localization of Tra-IR700 (TraIR). Scale bar, 30 μm. (**b**) Lysosomal localization of Tra-IR700 6 h after incubation. Scale bar, 50 μm. (**c**) Microscopic observation of before and after Tra-IR700 mediated photoimmunotherapy (PIT). Scale bar, 50 μm. (**d**) Irradiation dose dependent and target specific cell death in response to Tra-IR700 mediated PIT. Data are means ± s.e.m. (n = at least 4, *** $P < 0.001$ vs. non treatment control, Student's t test). (**e**) Long term growth inhibition in response to Tra-IR700 mediated

PIT. Data are means ± s.e.m. (n = 3, ** P < 0.01 vs. non treatment control, Student's t test). (**f**) Microscopic observation of growth inhibition in response to Tra-IR700 mediated PIT. Scale bar, 100 μm (**g**) Internalization of Tra-IR700 was not required for phototoxic cell death. Data are means ± s.e.m. (n = 3). (**h**) Target specific membrane binding of Tra-IR700 only induced phototoxic cell death. Data are means ± s.e.m. (n = 3). (**i**) HER2 negatively expressing A431 cells did not show phototoxic effects with Tra-IR700 mediated PIT (n = 3). (**j**) Sodium azide (NaN_3) concentration dependent inhibition of phototoxic cell death induced by Tra-IR700 mediated PIT. Data are means ± s.e.m. (n = 3, *** P < 0.001, ** P < 0.01 vs. 2.0 J cm^{-2} PIT treatment without NaN_3 control, Student's t test). DIC: differential interference contrast. PanIR: Pan-IR700.

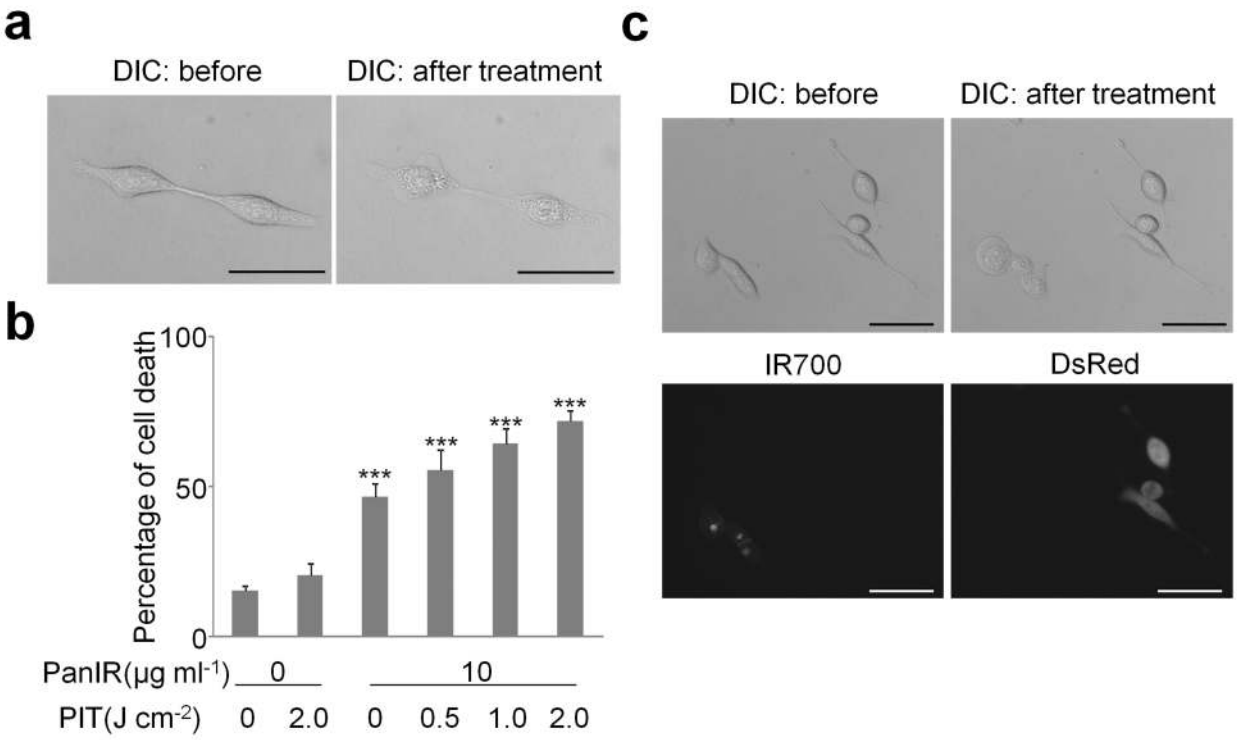

Figure 3. Target specific cell death in response to Pan-IR700 mediated photoimmunotherapy for EGFR expressing A431 cells

(**a**) Microscopic observation of before and after Pan-IR700 mediated photoimmunotherapy (PIT). Scale bar, 50 μm. (**b**) Irradiation dose dependent and target specific cell death in response to Pan-IR700 (PanIR) mediated PIT. Data are means ± s.e.m. (*n* = at least 4, *** $P < 0.001$ vs. non treatment control, Student's *t* test). (**c**) EGFR expressing cell specific necrotic cell death was induced by Pan-IR700 mediated PIT. Scale bar, 50 μm. DIC: differential interference contrast.

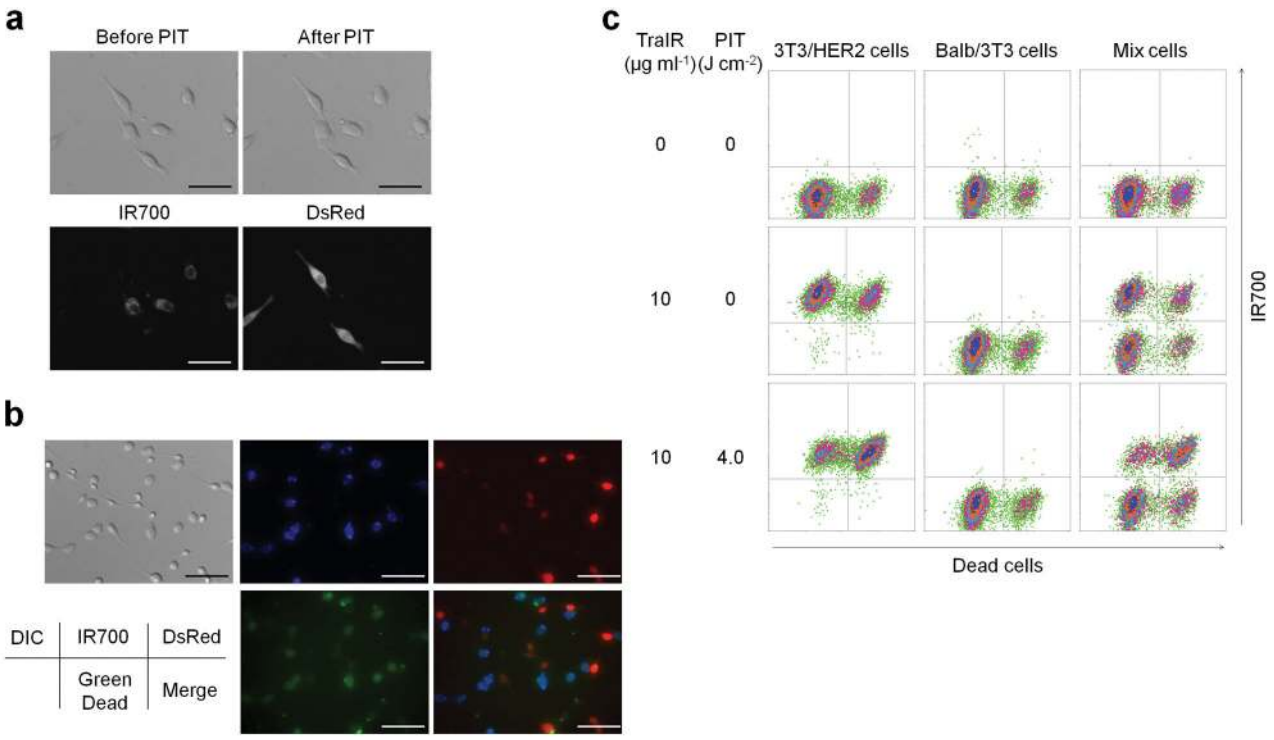

Figure 4. Tra-IR700 mediated photoimmunotherapy for HER2 expressing and non expressing co-cultured cells

(**a**) Induction of target specific photoimmunotherapy (PIT) lead to HER2 expressing cell specific necrotic cell death. Scale bar, 50 μm. (See also Supplementary Video 2) (**b**) HER2 specific cell death was confirmed with fluorescence microscopy with LIVE/DEAD Green staining. Scale bar, 100 μm. (**c**) Flow cytometric analysis for detecting HER2-specific cell death induced by Tra-IR700 (TraIR) mediated PIT. Upper left quadrant: Tra-IR700 positive, live cells; upper right quadrant; Tra-IR700 positive, dead cells; lower left quadrant: Tra-IR700 negative, live cells; lower right quadrant: Tra-IR700 negative, dead cells (n = 3). DIC: differential interference contrast.

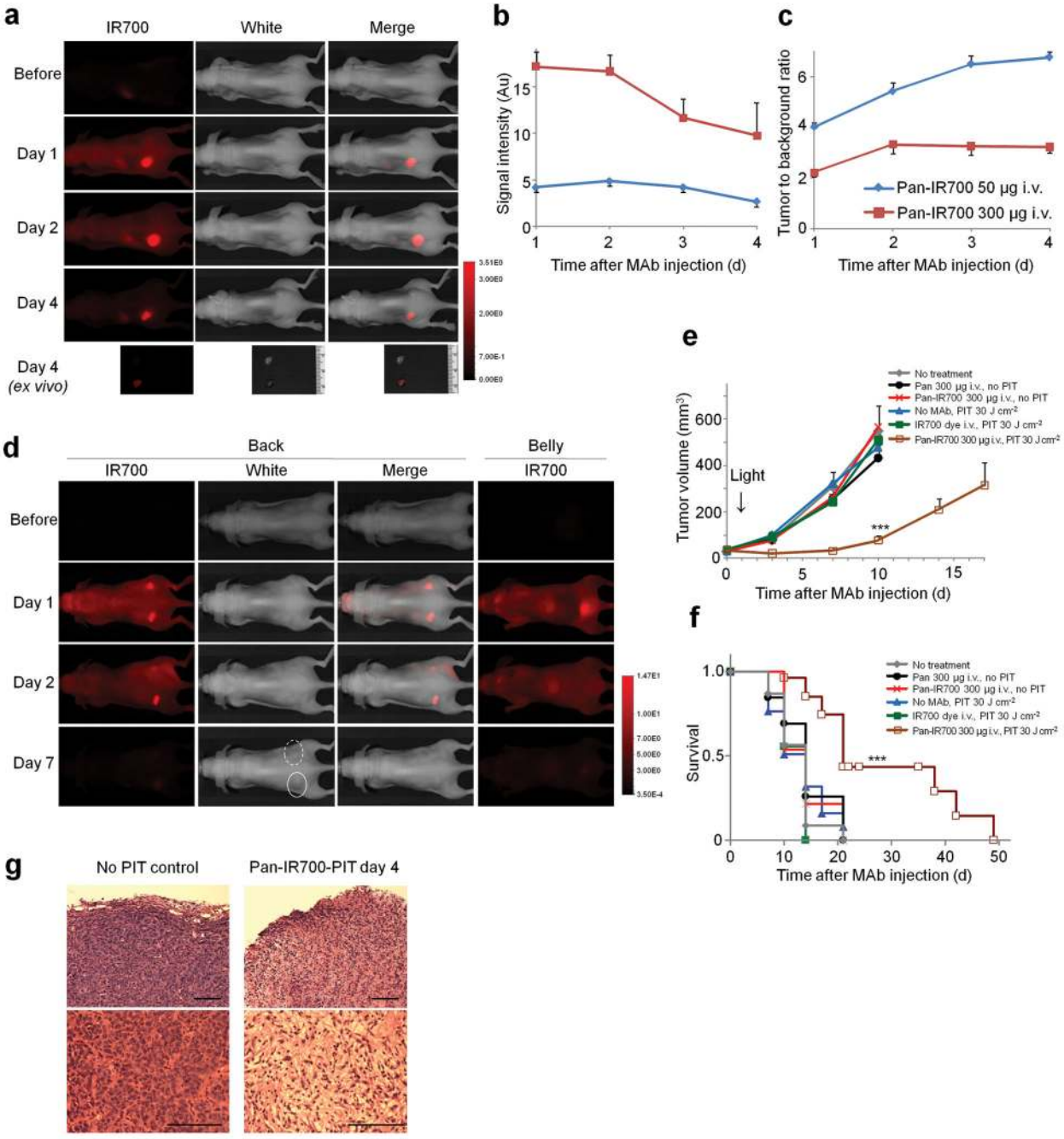

Figure 5. Pan-IR700 mediated photoimmunotherapy for HER1 expressing tumors *in vivo*

(**a**) HER1 positive A431 tumor (left dorsum) was selectively visualized as early as 1 d after Pan-IR700 injection (50 μg). HER1 negative 3T3/HER2 tumor (right dorsum) did not show detectable fluorescence ($n = 5$ mice). (**b**) Fluorescence intensity of IR700 in A431 tumors over time at two different dose of Pan-IR700. Data are means ± s.e.m. ($n = 4$ each mice). (**c**) Tumor to background ratio of IR700 fluorescence intensity in A431 tumors over time at two different dose of Pan-IR700. Data are means ± s.e.m. ($n = 4$ each mice). (**d**) Biodistribution of Pan-IR700. A431 tumors (both sides of dorsum) were selectively visualized with IR700

fluorescence as early as 1 d after Pan-IR700 injection (300 μg). Right side of the tumor was irradiated with near infrared (NIR) light on day 1, while left side of the tumor was covered with black tape. Tumor shrinkage was confirmed on day 7. Dashed line: irradiated tumor, solid line: non-irradiated tumor. (**e**) Target specific tumor growth inhibition by Pan-IR700 mediated photoimmunotherapy (PIT) for A431 tumors. PIT was performed on day 1 after Pan-IR700 injection (day 5 after tumor inoculation). Data are means ± s.e.m. (at least $n = 12$ mice in each group, *** $P < 0.001$ vs. other control groups, Kruskal–Wallis test with post-test). (**f**) Kaplan-Meier survival curve analysis of Pan-IR700 mediated PIT for A431 tumors (at least $n = 12$ mice in each group, *** $P < 0.001$ vs. other control groups, log-rank test with Bonferroni's correction for multiplicity). (**g**) Histological observation of treated and non-treated A431 tumors ($n = 5$ mice, hematoxylin and eosin staining). Scale bar, 100 μm. Pan: panitumumab.